MALAYSIAN JOURNAL OF MICROSCOPY

Journal homepage: https://malaysianjournalofmicroscopy.org

RESEARCH ARTICLE

PHOTOCATALYTIC PERFORMANCE OF TIO$_2$/ZNO COMPOSITES FOR EFFICIENT DEGRADATION OF METHYL ORANGE DYE: STRUCTURAL AND OPTICAL PROPERTIES

Hartini Ahmad Rafaie[1,2,*], Nurkhaizan Zulkepli[1], Nurul Fatahah Asyqin Zainal[1], Zul Adlan Mohd Hir[3], Hamizah Mokhtar[3]

[1]Centre of Foundation Studies, Universiti Teknologi MARA, Selangor Branch, Dengkil Campus, 43800 Dengkil, Selangor, Malaysia.
[2]Advanced Materials for Environmental Research Initiative Group, Universiti Teknologi MARA Perak Branch, Tapah Campus, 35400 Tapah Road, Perak, Malaysia.
[3]Faculty of Applied Sciences, Universiti Teknologi MARA Pahang, 26400 Bandar Tun Abdul Razak, Jengka, Pahang, Malaysia.

Abstract. Semiconductor-based photocatalysts, such as ZnO and TiO_2, are widely studied for the degradation of organic dyes in wastewater due to their stability and cost-effectiveness. However, ZnO alone suffers from rapid electron-hole recombination, limiting its photocatalytic performance, while TiO_2 is limited by UV-only activation. Herein, TiO_2/ZnO composites were synthesized with varying TiO_2 loadings (5 wt.%, 10 wt.%, and 15 wt.%) using an ultrasonic-assisted chemical mixing method. The structural, morphological, and optical properties were comprehensively characterized using scanning electron microscopy (SEM) coupled with energy-dispersive X-ray spectroscopy (EDX), Fourier-transform infrared spectroscopy (FTIR), and photoluminescence spectroscopy (PL). SEM showed that the 10 wt.% TiO_2/ZnO composite exhibited the most uniform dispersion and porous morphology. FTIR confirmed Ti–O–Zn bond formation, while PL spectra indicated that 10 wt.% TiO_2 incorporation achieved the lowest emission intensity, signifying reduced recombination. Photocatalytic degradation of methyl orange (5 mg/L) under UV irradiation (6 Watt, $\lambda = 325$ nm) demonstrated that the 10 wt.% TiO_2/ZnO composite achieved the highest efficiency (89.2 %) with a rate constant, k of 0.02106 min^{-1}, surpassing pure ZnO (82.6 %) and pure TiO_2 (74.4 %). In contrast, 15 wt.% TiO_2/ZnO composite caused agglomeration and increased recombination, lowering activity. These results confirm that optimization of TiO_2 loading enhances heterojunction formation, promotes charge separation, and, consequently, enhances photocatalytic efficiency. The findings indicate that TiO_2/ZnO composites with controlled composition hold great potential for sustainable wastewater treatment.

Keywords: Composites, methyl orange, photocatalyst, photocatalytic degradation, TiO_2/ZnO.

Article Info

Received 5 January 2026
Accepted 10 April 2026
Published 8 June 2026

***Corresponding author: hartinirafaie@uitm.edu.my**

ISSN: 1823-7010, eISSN: 2600-7444

1. INTRODUCTION

The rapid growth of the textile, pharmaceutical and chemical industries has significantly increased the discharge of dye-containing wastewater into the aquatic environment [1]. Methyl orange (MO), a common azo dye, is particularly concerned due to its chemical stability, toxicity, and resistance to biodegradation [2]. These persistent pollutants reduce light penetration in water bodies and pose serious risks to human health and ecosystem. Consequently, developing sustainable and environmentally friendly treatment technologies remains a global priority. While conventional methods like adsorption, coagulation and membrane filtration are effective, they offer from limitations [1, 2]. For instance, adsorption techniques primarily transfer pollutants from one phase to another without complete degradation, leading to secondary waste disposal issues [1]. Meanwhile, membrane filtration processes are hindered by high cost and fouling.

To achieve complete mineralization of organic pollutants, heterogeneous photocatalysis has emerged as a promising advanced oxidation process (AOPs). This eco-friendly method can degrade organic contaminants into harmless end products such as CO_2 and H_2O under light irradiation [3]. Among various materials, titanium dioxide (TiO_2) and zinc oxide (ZnO) are extensively studied owing to their abundance, chemical stability, non-toxicity, and strong oxidative capabilities. However, both have drawbacks where TiO_2 has a wide band gap (~3.2 eV) restricts light absorption in the UV range, which constitutes only about 4-5 % of the solar spectrum [4]. Conversely, ZnO possesses comparable band gap energy (~3.37 eV) and often exhibits higher electron mobility but suffers from rapid recombination rates of photogenerated charge carriers, reducing its overall efficiency [5].

Constructing heterojunction structures is an effective strategy to overcome these limitations. TiO_2/ZnO composites have attracted considerable attention due to their favorable band alignment, which facilitates the transfer of electrons and holes across the interface [6,7]. This separation prolongs the lifetime of charge carrier and enhances the generation of reactive species, such as hydroxyl radicals (OH) and superoxide anions (O_2^-), which drive the degradation process [7]. Recent studies emphasize that interfacial engineering and compositional tuning are critical for modulating charge carrier dynamics and surface reactivity [8,9].

Despite these advancements, optimizing the TiO_2 loading within ZnO matrices remains a challenge. Insufficient TiO_2 may not effectively establish a heterojunction interface, limiting charge separation efficiency, while excessive loading can lead to particle agglomeration, surface blockage and the formation of recombination centers [10]. These effects make it difficult to achieve an optimal balance between structural integration, surface area, light absorption and charge carrier dynamics. Although several studies have reported TiO_2/ZnO composites, systematic investigations correlating TiO_2 content with structural, optical and photocatalytic properties are still limited [8-10].

Therefore, this study systematically investigates the effect of TiO_2 loading (5, 10, 15 wt.%) on the structural, optical and photocatalytic properties of TiO_2/ZnO composites synthesized via an ultrasonic-assisted chemical mixing method. Characterization was performed using SEM-EDX, FTIR, PL, and UV-Visible spectroscopy. By establishing the relationship between composition, morphology and charge carrier behavior, this work identifies the optimal TiO_2 content for maximizing photocatalytic efficiency and provides deeper insights into the design of efficient heterostructure photocatalysts for wastewater treatment applications.

2. MATERIALS AND METHODS

Commercial zinc oxide (ZnO, 99 %) and titanium oxide (TiO_2, 99 %) were acquired from Sigma-Aldrich (Selangor, Malaysia). The chemicals used in this study were of analytical grade and all chemicals were used as received without further purification. Deionized (DI) water was used consistently during both the photocatalyst preparation and the photocatalytic testing. Methyl orange

(MO) from Sigma-Aldrich (Selangor, Malaysia), a model azo dye, was used as the target organic pollutant due to its representative structure and strong chromophoric absorbance at 466 nm.

2.1 Synthesis of TiO_2/ZnO Composites

The TiO_2/ZnO composite photocatalysts were prepared by an ultrasonic-assisted chemical mixing method to ensure uniform dispersion and intimate interfacial contact between TiO_2 and ZnO particles. Briefly, a known amount of ZnO and TiO_2 powder with different weight ratios were weighed and added into 100 mL of deionized (DI) water in a beaker. The suspension was subjected to an ultrasonication process for 60 minutes at room temperature using an ultrasonicator (SONICS Vibra-Cell, 20 kHz, 750 W) to obtain homogeneous dispersion of the particles and initiate initial mixing. This was followed by continuous magnetic stirring for 2 hours to enhance the interfacial interaction between ZnO and TiO_2 particles. The suspensions were subsequently dried at 100 °C for 24 hours in a conventional oven to obtain dry composite powders. The dried powders were then ground to fine particles with an agate mortar and pestle and then kept in sealed containers for subsequent characterization and photocatalytic testing. To investigate the synergistic effects between ZnO and TiO_2, different weight ratios of TiO_2 as shown in Table 1 were prepared under the same conditions while pure ZnO and TiO_2 were used for comparison purposes.

Table 1: Composition of TiO_2/ZnO composites

Sample ID	ZnO (g)	TiO_2 (g)	TiO_2 Loading (wt.%)
Pure ZnO	4.00	0	0
Pure TiO_2	0	4.00	0
5 wt.% TiO_2/ZnO	3.80	0.20	5
10 wt.%TiO_2/ZnO	3.60	0.40	10
15 wt.% TiO_2/ZnO	3.40	0.60	15

2.2 Characterization Techniques

The structural and optical characteristics of the synthesized photocatalysts were analyzed using various analytical techniques. The morphology of the samples was examined by using a scanning electron microscope (SEM, TESCAN VEGA 3) equipped with an energy-dispersive X-ray (EDX) detector. Fourier-transform infrared (FTIR) spectroscopy was utilized to identify chemical bonds and functional groups within the range of 4000–400 cm^{-1}. Photoluminescence (PL) spectra were obtained using a JASCO FP-8500 Spectrofluorometer in the range of 350–750 nm at an excitation wavelength of 320 nm. UV–Visible absorbance spectra were recorded for photocatalytic degradation in the range of 300–700 nm, with methyl orange (MO) degradation monitored at 466 nm. These combined techniques provided valuable insights into the physicochemical properties that influence the photocatalytic performance of the TiO_2/ZnO composites.

2.3 Photocatalytic Evaluation

Photocatalytic degradation experiments under UV irradiation were performed to evaluate the performance of the synthesized composites. Figure 1 illustrates the experimental setup for photocatalytic degradation experiment. In a typical procedure, 20 mg of photocatalyst was dispersed in 100 mL of 5 mg/L MO dye solution contained in a 250 mL beaker. The suspension was magnetically stirred in the dark for 30 minutes to allow adsorption-desorption equilibrium between the catalyst surface and MO dye molecules. After equilibration, the suspension was exposed to a 6-Watt UV lamp (λ = 325 nm, positioned 10 cm above the surface). The light intensity was not directly measured; however, the experimental conditions were kept constants for all samples to ensure valid comparison. During the irradiation process, 5 mL samples were collected at 10-minute intervals over a 90-minute period. Each sample was centrifuged at 5000 rpm for 5 minutes to remove any residual catalyst particles, and the supernatant was analyzed by using UV-Visible spectroscopy to measure the MO concentration.

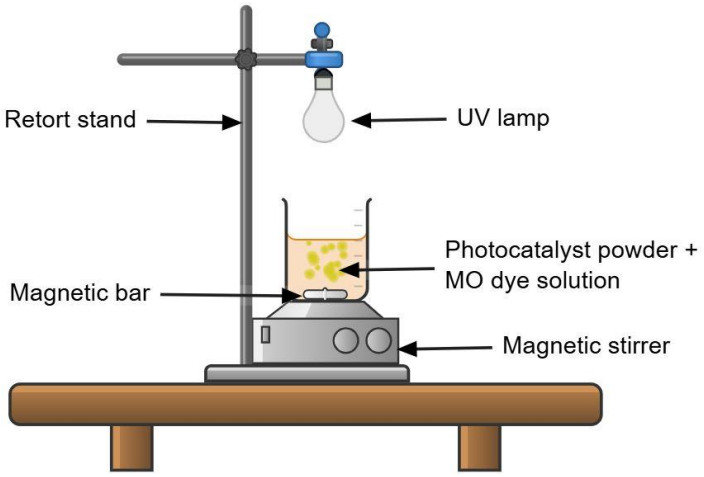

Figure 1: Experimental setup for catalytic photodegradation of methyl orange (MO)

The dye degradation efficiency was calculated using the following equation [11]:

$$Degradation\ Efficiency\ (\%) = \frac{C_0 - C_t}{C_0} \quad (1)$$

where C_t is the dye concentration at time t, and C_0 is the initial concentration at time 0. The initial concentration (C_0) was defined after the 30-minute dark adsorption-desorption equilibrium period, and this point was considered as t = 0, corresponding to the onset of UV irradiation. The degradation kinetics were analyzed using the pseudo-first-order kinetic model:

$$\ln\left(\frac{C_0}{C_t}\right) = kt \quad (2)$$

where k is the apparent rate constant, and t is the irradiation time.

3. RESULTS AND DISCUSSION

3.1 Morphological and Elemental Composition

The surface morphologies and microstructural characteristics of pure ZnO, pure TiO2 and the synthesized TiO_2/ZnO composites were examined using scanning electron microscopy (SEM), while the elemental composition was analyzed through energy-dispersive X-ray spectroscopy (EDX). Figure 2 displays the surface morphologies of pure ZnO, pure TiO_2, and TiO_2/ZnO composites at 1000x and 5000x magnification.

Pure ZnO (Figures 2(a) and 2(b)) exhibited irregular, agglomerated particles with rough surfaces, a typical feature of oxide nanoparticles with high surface energy. Such aggregation can limit photocatalytic efficiency by reducing the available surface area [7]. On the other hand, pure TiO_2 displayed smaller, more uniform grains with a smoother texture (Figures 2(c) and 2(d)). With TiO_2 incorporation, the surface morphology of ZnO gradually changed. As can be depicted in Figures 2(e) and 2(f), the 5 wt.% TiO_2/ZnO composites show a slight decreased in agglomeration, resulting in better particle dispersion. Upon further increases in the TiO_2 content, the 10 wt.% TiO_2/ZnO composite exhibited the most optimal morphology, featuring denser coverage and improved porosity as evident from Figures 2(g) and 2(h). This indicates that TiO_2 was evenly distributed throughout the ZnO matrix, resulting in a larger effective surface area and more active sites for dye adsorption and degradation. Similar morphological improvements through compositional tuning have been reported in recent heterostructure studies, where optimized loading prevents the self-aggregation of individual phases

[2,7]. In contrast, at a 15 wt.% TiO_2 loading, an excess of TiO_2 caused aggregation and surface blockage, which creates a shadowing effect that hinders light penetration and reduces the photocatalytic efficiency (Figures 2(i) and 2(j)) [6,10].

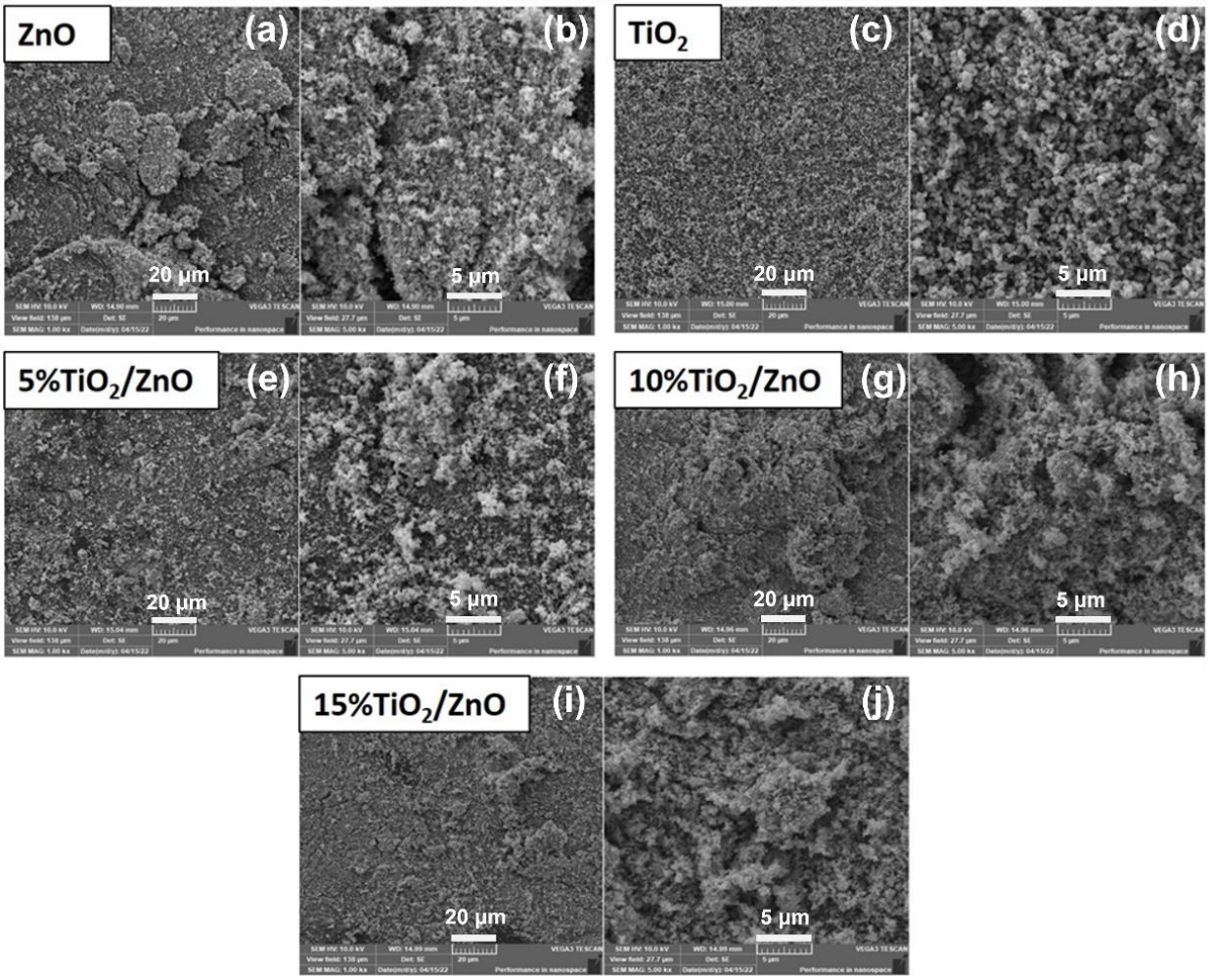

Figure 2: SEM micrographs of (a)-(b) pure ZnO, (c)-(d) pure TiO_2, (e)-(f) 5 wt.%, (g)-(h) 10 wt.%, and (i)-(j) 15 wt.% TiO_2/ZnO composites at magnifications of 1000x (a, c, e, g, i) and 5000x (b, d, f, h, j)

Figure 3 depicts EDX elemental mapping of pure ZnO, pure TiO_2 and 10 wt.% TiO_2/ZnO composites that confirmed the presence and homogeneous distribution of Zn, Ti, and O elements across all composites. In addition, no foreign impurities were detected, confirming the purity of the synthesized materials. Uniform Ti dispersion is particularly crucial because localized Ti clusters could act as recombination centers, whereas homogeneity enhances interfacial contact and promotes efficient charge transfer between ZnO and TiO_2. The homogeneous distribution of Ti across ZnO particles enhanced interfacial charge transfer, consistent with recent reports [12].

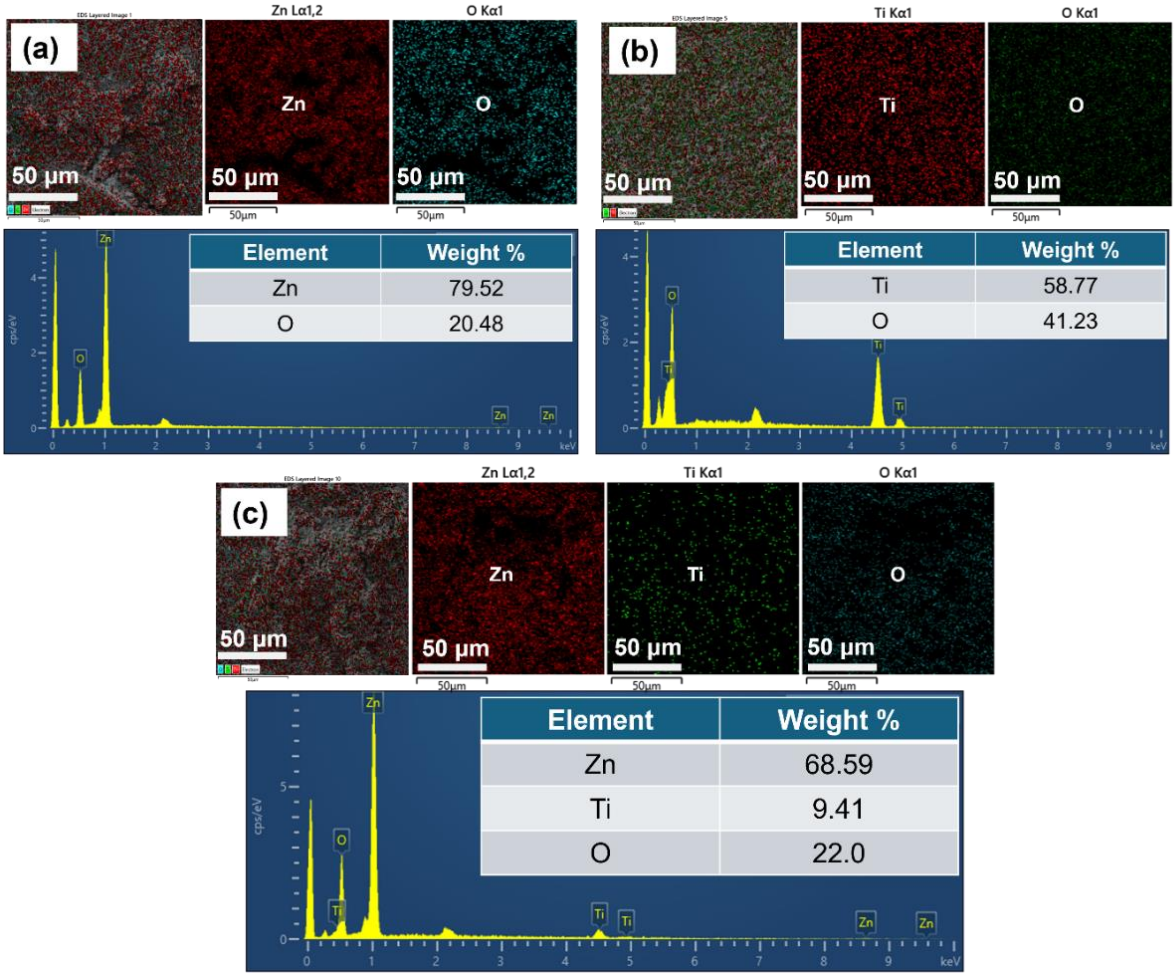

Figure 3: EDX analysis, along with elemental mapping and spectra of (a) pure ZnO, (b) pure TiO_2, and (c) 10 wt.% TiO_2/ZnO composites prepared via the chemical mixing method

3.2 Functional Group and Bonding Characterization (FTIR) Analysis

For the FTIR study, pure ZnO, pure TiO_2, and the optimized 10 wt.% TiO_2/ZnO composite were chosen as representative samples. This selection emphasizes the key chemical interactions and heterojunction formation at the most effective loading while allowing a direct comparison with the individual base materials. The 5 wt.% and 15 wt. composites were excluded in the spectra to avoid redundancy, as they exhibited comparable functional group features. Accordingly, Figure 4 presents the FTIR spectra of pure ZnO, pure TiO_2 and the selected 10 wt.% TiO_2/ZnO composites in the range 400 – 4000 cm^{-1}. A strong absorption band at around 540 cm^{-1}, assigned to Zn–O stretching vibrations was seen for pure ZnO [13]. Meanwhile, pure TiO_2 exhibits characteristic Ti–O–Ti and Ti–O vibrations in the region of 470–600 cm^{-1}. For the 10 wt % TiO_2/ZnO composites, bands are detected at around 536 and 676 cm^{-1}, which are attributed to Ti–O and Ti–O–O vibrations, respectively. The overlap and slight variation of the Zn–O and Ti–O bonds suggest possible interactions between the two oxides components, potentially indicating the formation of Ti–O–Zn linkages and minor lattice distortion. These interfacial interactions are associated with heterojunction formation, which facilitates charge transfer across the semiconductor interface.

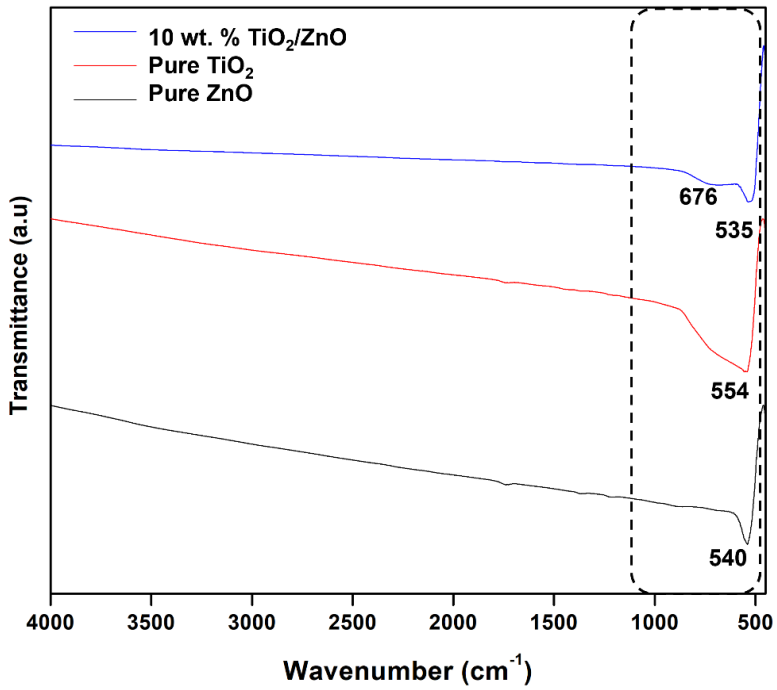

Figure 4: FTIR spectrum of pure ZnO, pure TiO_2 and 10 wt.% TiO_2/ZnO composites

3.3 Photoluminescence Analysis

Photoluminescence (PL) spectra provided insights into charge recombination behavior. Figure 5 shows the near-band-edge (NBE) emission peak in pure ZnO around 380 nm, which is attributed to excitonic recombination, along with additional visible emissions associated with oxygen vacancies. The high PL intensity signifies a substantial electron–hole recombination, which limits photocatalytic efficiency.

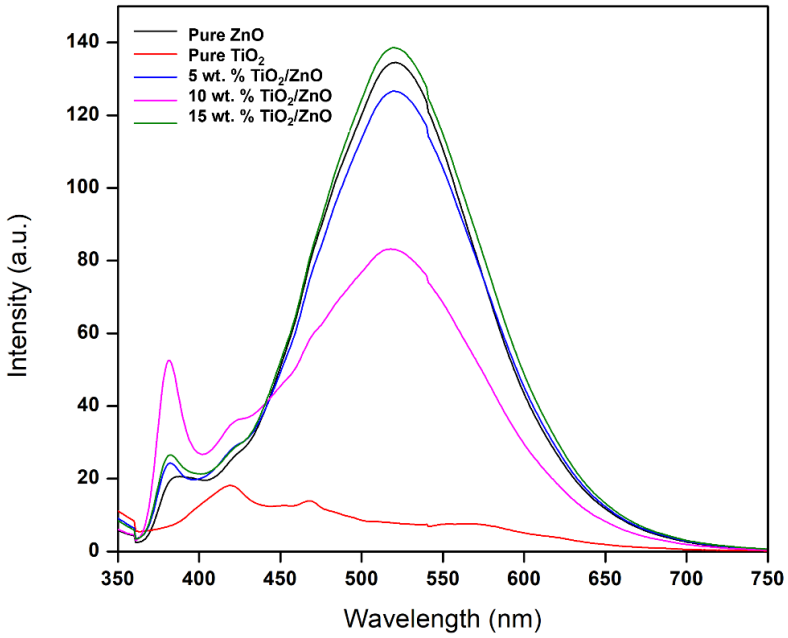

Figure 5: PL spectra of pure ZnO, pure TiO_2, 5 wt.%, 10 wt.% and 15 wt.% TiO_2/ZnO composites

In contrast, pure TiO_2 displayed very weak PL emission, suggesting low electron-hole recombination but also limited photoactivity under UV irradiation due to its wider band gap. For the 5 wt.% TiO_2/ZnO composite, the PL intensity was decreased compared with that of pure ZnO, indicating a partial suppression of recombination. At 10 wt.% loading, PL reached its lowest intensity, indicating the most efficient charge separation and the most effective heterojunction formation [14]. However, at 15 wt.%, PL intensity was found to increase again, suggesting that excessive TiO_2 introduced recombination centers or caused shielding effects that suppressed light absorption. Interestingly, a slight blue shift in emission peaks was observed with higher TiO_2 contents. This behavior can be attributed to lattice strain induced by the incorporation of Ti^{4+} ions into the ZnO lattice, leading to distortion of the crystal structure and modification of the electronic band structure. Such lattice distortion can alter defect energy levels and reduce the density of deep-level defect states, resulting in a shift of emission toward shorter wavelengths. In addition, the formation of a TiO_2-ZnO heterojunction may influence charge distribution at the interface, further contributing to band structure modulation. Similar blue shift phenomena have been reported in ZnO-based composite system, where interfacial strain and defects led to band gap widening and emission peak shifts [3, 14]. This suggests that TiO2 incorporation not only suppresses charge recombination but also plays a role in tailoring the electronic and defect structure of ZnO.

3.4 Photocatalytic Performance Evaluation

The photocatalytic degradation of MO was assessed using pure ZnO, pure TiO_2, and TiO_2/ZnO composite photocatalysts by monitoring the degradation under ultraviolet (UV) irradiation for 90 minutes. Prior to UV irradiation, the suspension was stirred in the dark for 30 minutes to establish adsorption-desorption equilibrium between the photocatalyst surface and methyl orange (MO) molecules, ensuring that subsequent degradation is primarily attributed to photocatalytic reactions rather than initial adsorption [3, 6]. The concentration measured at the end of this dark period was defined as the initial concentration (C_0), corresponding to t =0), which marks the onset of the UV irradiation. Therefore, the degradation profile presented in this study reflects the photocatalytic activity under UV light. Although adsorption may contribute to initial dye removal, its extent was not separately quantified in this work. As shown in Figure 6(a), pure ZnO achieved 82.6 % degradation within 90 minutes, while pure TiO_2 degraded 74.4 %. The composites outperformed both pure oxide samples, with the 10 wt.% TiO_2/ZnO composites sample achieving the highest degradation efficiency of 89.2 %, respectively. The 5 wt.% TiO_2/ZnO composites obtained 83.60 % degradation compared to pure ZnO and TiO_2, while composites with 15 wt.% TiO_2 showed diminished performance at 55.50 %, respectively.

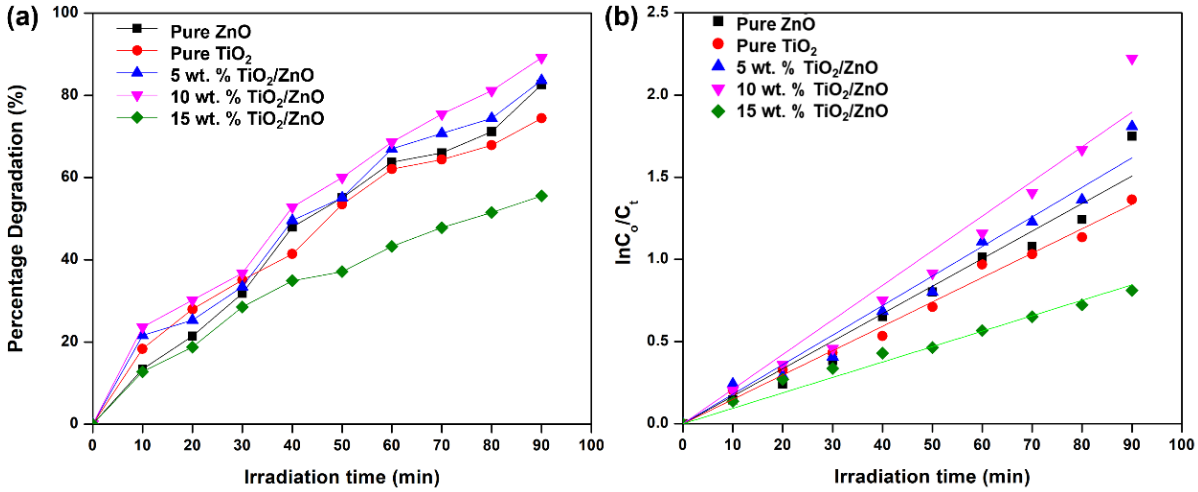

Figure 6: (a) Comparison of MO dye degradation percentages after 90 minutes of irradiation, and (b) linear kinetic fit for MO dye photodegradation using different TiO_2/ZnO composite photocatalysts

The enhanced performance of the 10 wt.% TiO_2/ZnO composite can be attributed to the balance between sufficient TiO_2 content to form effective heterojunctions and minimal aggregation, as supported by SEM and PL analyses. SEM micrographs showed that the 10 wt.% TiO_2/ZnO composite sample had a relatively homogenous dispersion of the particles with less surface agglomeration compared to the sample with more TiO_2 loading, which enables better light penetration and, consequently a higher effective surface area. The formation of well-integrated ZnO–TiO_2 interfaces was observed, which played a significant role in promoting the separation of photo-induced charge carriers. EDX analysis further confirmed the homogeneous distribution of Ti in the ZnO matrix, without the trace of secondary phases or contaminants, indicating successful compositional integration. Furthermore, FTIR spectroscopy further validated the coexistence of Zn–O and Ti–O stretching vibrations within the composite, while slight band shifts suggested defect-rich regions and potential lattice distortion due to TiO_2 incorporation. These surface defects enhance dye molecule adsorption and facilitate the formation of reactive oxygen species during photocatalysis. Additionally, the photoluminescence spectrum of the 10 wt.% TiO_2/ZnO composite displayed a moderate emission intensity compared to the other samples, suggesting efficient suppression of electron–hole recombination. This implies a favorable charge transfer process across the ZnO–TiO_2 heterojunction, which is essential for sustaining redox reactions during dye degradation. In contrast, further increasing the doping amount of TiO_2 up to 15 wt.% decreased the photocatalytic efficiency which might be due to excess of TiO_2 particles acting as recombination centers or physically block the active sites of ZnO [15]. At higher TiO_2 loading, particle agglomeration can induce a shadowing effect, where UV light penetration into the suspension is hindered, reducing effective photon utilization and limiting photocatalytic efficiency. These factors, along with the poor dispersion seen in SEM images and lower PL emission intensities, collectively hinder the generation of reactive species required for dye degradation. Overall, the superior performance of the 10 wt.% TiO_2/ZnO composites photocatalyst demonstrates that appropriate TiO_2 loading enhances interfacial interaction, light harvesting, charge separation, and surface reactivity [16]. This finding underscores the importance of compositional tuning and structural optimization in designing effective photocatalysts for wastewater treatment applications.

3.5 Kinetic Analysis

The reaction kinetics of MO degradation over the prepared photocatalysts was evaluated using a pseudo-first-order kinetics model, as illustrated in Figure 6(b). A strong linear relationship between $\ln(C_0/C_t)$ and irradiation time was observed for all samples, indicating the degradation process follows pseudo-first-order kinetics. Notably, the apparent rate constant of the 10 wt.% TiO_2/ZnO composite achieved the highest apparent rate constant ($k = 0.02106\ min^{-1}$), indicating its superior photocatalytic efficiency. This rate constant of 10 wt.% TiO_2/ZnO composite was substantially higher compared to those of pure ZnO ($k = 0.01675\ min^{-1}$), pure TiO_2 ($k = 0.01483\ min^{-1}$), and the 5 wt.% TiO_2/ZnO composite ($k = 0.01798\ min^{-1}$). The improved kinetics performance of the 10 wt.% composite is consistent with the earlier structural and optical analyses, which revealed improved morphology, reduced electron-hole recombination, and uniform elemental distribution. In contrast, the 15 wt.% TiO_2/ZnO composite showed a significant decrease in photocatalytic activity, with a lower rate constant of $k = 0.009390\ min^{-1}$ [8, 17]. The lower rates at higher doping levels might be attributed to increased particle agglomeration, with excess TiO_2 serving as recombination centers or causing light shielding, as supported by the SEM and PL results. To further assess the applicability of the kinetic model, the correlation coefficients (R^2) values for all photocatalysts were determined and are presented in Table 2. The R^2 for each sample exceeding 0.98, confirming good agreement with the pseudo-first-order kinetics model. Moreover, the kinetic data clearly reinforce the conclusion that 10 wt.% TiO_2 loading provides the most effective configuration for enhancing photocatalytic activity through balancing structural integration, charge carrier dynamics, and surface accessibility.

Table 2: Photocatalytic degradation efficiency, apparent rate constant (k), and correlation coefficient (R^2) for methyl orange degradation using pure ZnO, pure TiO_2, and TiO_2/ZnO composite photocatalysts

Sample ID	Percentage Degradation (%)	Photodegradation Rate constant, k (min^{-1})	R^2 value
Pure ZnO	82.60	0.01675	0.98596
Pure TiO_2	74.40	0.01483	0.99676
5 wt.% TiO_2/ZnO	83.60	0.01798	0.99035
10 wt.%TiO_2/ZnO	89.20	0.02106	0.98408
15 wt.% TiO_2/ZnO	55.50	0.00939	0.99279

*R^2: Correlation coefficient obtained from pseudo-first-order kinetic fitting.

3.6 Photocatalytic mechanism

The enhanced photocatalytic activity of the TiO_2/ZnO composite is attributed to the formation of a heterojunction structure that promotes efficient charge separation [6, 7]. Upon UV irradiation, both TiO_2 and ZnO generate electro-hole (e^-/ h^+) pairs as shown in Figure 7. Due to favorable band alignment, electrons from the conduction band of ZnO transfer to TiO_2, while holes migrate in the opposite direction, effectively suppressing recombination, as supported by PL results [6, 8].

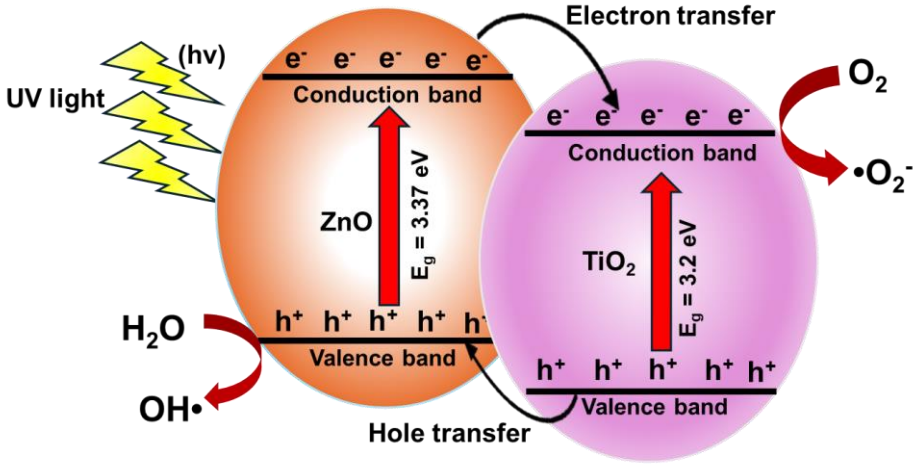

Figure 7: Proposed photocatalytic mechanism of TiO_2/ZnO composite

The separated electrons react with dissolved oxygen to form superoxide radical (O_2^-), while holes oxidize water or hydroxide ions to produce hydroxyl radicals (OH), which are responsible for the degradation of methyl orange [3, 7]. The optimum TiO_2 loading (10 wt.%) provides sufficient interfacial contact without excessive agglomeration, leading to improve light absorption and enhanced generation of reaction species.

4. CONCLUSIONS

In this study, TiO_2/ZnO composites were successfully synthesized via a simple ultrasonic-assisted chemical mixing method and evaluated for their photocatalytic performance was assessed toward the degradation of methyl orange (MO) dye under UV irradiation. Comprehensive characterization by SEM-EDX, FTIR, PL, and UV–Visible spectroscopy demonstrated that the structural integration of TiO_2 into ZnO significantly influenced the morphology, surface chemistry, and

charge carrier dynamics of the composites. Among the prepared samples, the 10 wt.% TiO_2/ZnO composite exhibits the highest photocatalytic activity, with a degradation efficiency of 89.20 % and an apparent rate constant, k of 0.02106 min^{-1}. This enhancement in photocatalytic activity was attributed to the enhanced interfacial contact between TiO_2 and ZnO, reduced electron-hole recombination, and defect sites that promoted reactive species generation. A further increase in TiO_2 loadings up to 15 wt.% resulted in a decreased photocatalytic performance due to surface agglomeration and light scattering, providing more recombination centers. These results highlight the influence of compositional tuning in heterostructure photocatalysts and confirm the existence of an optimal TiO_2 content is crucial for achieving high photocatalytic efficiency. These results contribute valuable insights into the structure and activity relationship of metal oxide composites and support the potential application of TiO_2/ZnO composites in the treatment of dye-contaminated wastewater.

Acknowledgements

The authors gratefully acknowledge KWEF Grant (Project No: 100-TNCPI/INT 16/6/2 (046/2024)), Universiti Teknologi MARA (UiTM) Shah Alam and Pahang Branch for providing the facilities to carry out the research work, management, and technical support.

Author Contributions

All authors contributed toward data analysis, drafting and critically revising the paper and agree to be accountable for all aspects of the work.

Disclosure of Conflict of Interest

The authors have no disclosures to declare.

Compliance with Ethical Standards

The work is compliant with ethical standards.

References:

[1] Makhwedzha, D. R., Henry, A., Moropeng, M. L. & Mbaya, R. (2022). Activated carbon derived from waste orange and lemon peels for the adsorption of methyl orange and methylene blue dyes from wastewater. *Heliyon, 127*, 1-9.

[2] Mensah, K.,Shokry, H., Elkady, M., Hawash, H. B. & Samy, M. (2024). Enhanced photocatalytic degradation of dyes using a novel waste tonerbased TiO_2/Fe_2O_3@nanographite nanohybrid: A sustainable approach. *Water Science and Engineering*, 17(3), 226–235.

[3] Nemiwal, M., Zhang, T. C. & Kumar, D. (2021). Recent progress in g-C_3N_4, TiO_2 and ZnO based photocatalysts for dye degradation: Strategies to improve photocatalytic activity. *The Science of The Total Environment*. *767*, 144896.

[4] Hossain, M. K., Hossain, M. M. M. & Akhtar, S. (2023). Studies on synthesis, characterization, and photocatalytic activity of TiO_2 and Cr-doped TiO_2 for the degradation of p-Chlorophen. *ACS Omega*, 8(2), 1979–1988.

[5] Peerakiatkhajohn, P., Butburee, T., Sul, J., Thaweesak, S. & Yun, J. (2021). Efficient and rapid photocatalytic degradation of methyl orange dye using Al/ZnO nanoparticles. *Nanomaterials*. 11(4), 1059.

[6] Ghamarpoor, R., Fallah, A. & Jamshidi, M. (2024). A review of synthesis methods, modifications, and mechanisms of ZnO/TiO_2-based photocatalysts for photodegradation of contaminants. *ACS Omega*, 9(24), 25457-25492.

[7] Kumar, A., Nayak, D., Sahoo, P., Nandi, B. K., Saxena, V. K. & Thangavel, R. (2023). Fabrication of porous and visible light active ZnO nanorods and ZnO@TiO_2 core-shell photocatalysts for self-cleaning applications. *Physical Chemistry Chemical Physics*, 25(24), 16423-16437.

[8] Dai, J., Wu, Y., Yao, Y. & Zhang, B. (2025) ZnO/TiO_2 photocatalysts for degradation of methyl orange by low-power irradiation. *Science Progress*, 108(1), 1-25.

[9] Kighuta, K., Gopalan, A. I., Lee, D., Saianand, G., Hou, Y., Park, S., Lee, K., Lee, J. & Kim, W. (2021). Optimization and modeling of efficient photocatalytic TiO_2-ZnO composite preparation parameters by response surface methodology. *Journal of Environmental Chemical Engineering*. 9(6), 106417.

[10] Mapukata, S. & Nyokong, T. (2020). Development of phthalocyanine functionalised TiO_2 and ZnO nanofibers for photodegradation of methyl orange, *New Journal of Chemistry,* 44(38), 16340-16350.

[11] Suneel, M. A. K., Tabassum, N., Khan, A. R., Feroz, Z. & Rahman, Q. I. (2025). Synthesis and photocatalytic performance of g-C_3N_4/ZnO Nanocomposites for the efficient degradation of dyes under sunlight. *Environmental and Earth Sciences Proceedings*, 32(1), 18.

[12] Elsellami, L. & Djeridi, W. (2022). Charge transfer modulation (e−/h+) between TiO_2, ZnO, and Ag for a superior photocatalytic performance. *Journal of Materials Research*, 37(4), 897-908.

[13] Ali, M., Aissa, B., Khairy, M., Khalifa, M. E., Abdelrahman, E. A., Raza, N., Masoud, E. M. & Modwi, A. K. (2024). Facile synthesis of TiO_2@ZnO nanoparticles for enhanced removal of methyl orange and indigo carmine dyes: Adsorption, kinetics. *Heliyon*. 10(10), 31351.

[14] Nawaz, R., Ullah, H., Ghanim, A. A., Irfan, M., Anjum, M., Rahman, S., Ullah, S., Abdel Baki, Z. & Kumar Oad, V. (2023). Green synthesis of ZnO and black TiO_2 materials and their application in photodegradation of organic pollutants. *ACS Omega,* 8(39), 36076 - 36087.

[15] Dele-Afolabi, T. T., Azmah Hanim, M. A., Oyekanmi, A., Ansari, M., Sikiru, S. & Ojo-kupoluyi, O.J. (2024). Organic waste-derived pore formers for macroporous ceramics fabrication: A review on synthesis, durability properties and potential applications. *Materials Today Sustainability*. (27), 100824.

[16] Taghizadeh-Lendeh, P., Mohsen Sarrafi, A. H., Alihosseini, A., & Bahri-Laleh, N. (2023). Synthesis and characterisation ZnO/TiO_2 incorporated activated carbon as photocatalyst for gas refinery effluent treatment. *Polyhedron*. (247), 116715.

[17] Landge, V. K., Huang, C., Hakke, V. S., Sonawane, S. H., Manickam, S. & Hsieh, M. C. (2022). Solar-energy-driven Cu-ZnO/TiO_2 nanocomposite photocatalyst for the rapid degradation of congo red azo dye. *Catalysts*. 12(6), 605.